

Electronic Properties of Water in Liquid Environment. A Sequential QM/MM Study Using the Free Energy Gradient Method

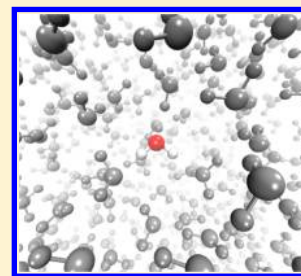
Herbert C. Georg*

Instituto de Física, Universidade Federal de Goiás, CP 131, 74001-970, Goiânia, GO, Brazil

Sylvio Canuto

Instituto de Física, Universidade de São Paulo, CP 66318, 05314-970, São Paulo, SP, Brazil

ABSTRACT: There is a continuous search for theoretical methods that are able to describe the effects of the liquid environment on molecular systems. Different methods emphasize different aspects, and the treatment of both the local and bulk properties is still a great challenge. In this work, the electronic properties of a water molecule in liquid environment is studied by performing a relaxation of the geometry and electronic distribution using the free energy gradient method. This is made using a series of steps in each of which we run a purely molecular mechanical (MM) Monte Carlo Metropolis simulation of liquid water and subsequently perform a quantum mechanical/molecular mechanical (QM/MM) calculation of the ensemble averages of the charge distribution, atomic forces, and second derivatives. The MP2/aug-cc-pV5Z level is used to describe the electronic properties of the QM water. B3LYP with specially designed basis functions are used for the magnetic properties. Very good agreement is found for the local properties of water, such as geometry, vibrational frequencies, dipole moment, dipole polarizability, chemical shift, and spin–spin coupling constants. The very good performance of the free energy method combined with a QM/MM approach along with the possible limitations are briefly discussed.



1. INTRODUCTION

Water is both one of the most important and one of the most common substances in earth. It has a very simple molecular structure. Nevertheless, a number of interesting properties arise when many water molecules come together.¹ It is by far the champion substance in the number of anomalies, many of them with important implications to life. It is perhaps the most studied substance, but still there is not a completely satisfactory theoretical model to treat bulk water.

Common approaches for simulating water in condensed phase using molecular dynamics (MD) or Monte Carlo (MC) may be classified in three types: fully quantum (QM), fully classical (MM) and mixed quantum-classical (QM/MM). The QM approach is satisfactory because of its generality (as no empirically fitted parameter is needed) as well as the possibility to cover a wide range of phenomena (as the electronic motion is also taken into account). However, the price for such high level approach is a very high computational demand that imposes some severe limitations on the size of the system. Ab initio simulations of liquid water are typically limited to a relatively small number of molecules even for large computer resources. Also, generally, only a small total time span is realistic at present times. There is a continuous increase in the developments and applications of QM/MM methods.^{2,3} Indeed, the use of a QM/MM approach in different problems in molecular and biomolecular systems has shown its feasibility and accuracy.^{2,3} It is indispensable for several problems in molecular and biomolecular systems. In this sense, much

attention has been devoted to the theoretical study of the properties of a reference molecule in the presence of other molecules treated as a solvent. In particular, water has deserved special attention.^{4–8}

For instance, Moriarty and Karlström⁴ have performed a geometry optimization of a reference water molecule in liquid environment using a conventional QM/MM approach in which the reference water was treated at the Hartree–Fock (HF) level. It is known experimentally that both the O–H bond and the H–O–H angle increase from gas to liquid phase. Their results show the same trend, but their O–H bonds are a little underestimated, and the H–O–H angle is a little overestimated. Certainly, those results are affected by the lack of accuracy of the HF method for calculating the molecular geometry and charge distribution.

Nymand and Åstrand⁵ have also optimized the geometry of water in liquid environment. They used the CASSCF method to treat the central water embedded in the electric field (ensemble averaged) of the surrounding water molecules represented by point charges. The ensemble of solvent water was obtained with a single MD simulation using the polarizable NEMO potential⁹ and keeping all the water molecules in rigid gas-phase geometry. They have found an equilibrium in-liquid geometry that is in good accord with the experimental

Received: May 1, 2012

Revised: August 10, 2012

Published: August 15, 2012



estimate,¹⁰ but other properties such as vibrational frequencies⁵ and NMR chemical shift⁶ are not well described. This may be caused, in part, by the lack of a more accurate description of the environment around the relaxed reference water molecule.

Finally, Chalmet and Ruiz-López⁷ also performed geometry optimization of a water molecule in liquid environment using a density functional theory (DFT) method to describe the reference molecule in a QM/MM simulation with MD (called Model 3 in their paper). They found an induced dipole for the in-liquid water molecule of ~ 0.8 D, which is in good agreement with theoretical and experimental estimates,¹¹ but the employed DFT method overestimates the O–H bond length and dipole moment of both the isolated and in-liquid molecule.

In the present work, our goal is to describe the electronic structure of a reference water molecule in liquid environment. Aiming at a higher accuracy, we follow different simulation and optimization approaches and also employ a higher QM level, namely MP2/aug-cc-pV5Z. We thus applied the free energy gradient method,¹² together with the average solvent electrostatic configuration¹³ (ASEC), which is a realistic mean field approach to the solvent effect, to describe the equilibrium electronic properties of the water molecule in liquid environment. We focus on the geometry, dipole moment, dipole polarizability, infrared spectrum, NMR chemical shift, and spin–spin coupling constant (SSCC).

In a recent paper¹⁴ we applied this methodology to study the NMR parameters of liquid ammonia, considering the importance of both electronic polarization and geometry relaxation of the ammonia molecule. Applying the free energy gradient method¹² together with the polarization scheme¹⁵ and the ASEC approach to describe the solvent average field,¹³ we could describe well the SSCC $^1J(^{15}\text{N},\text{H})$ of ammonia in liquid phase, and even better the gas-to-liquid shift. However, the gas-to-liquid shift of the spin–spin coupling is relatively small for ammonia. A better test for the accuracy of the methodology would be the description of the water molecule in liquid phase. Therefore, the present work tests the accuracy of the QM/MM free energy gradient methodology for obtaining accurate in-liquid molecular properties and spectra.

2. METHODOLOGY

We are interested in the local properties of water molecules in liquid environment. To investigate that, we performed a series of simulations in which one reference water molecule is surrounded by 500 solvent water molecules. In this series of simulations, we iteratively relax the charge distribution and the geometry of the reference, central water, employing, at each step, the sequential QM/MM methodology.¹⁶

Each step of such iterative relaxation consists of a simulation in which all the molecules are treated classically (that is, all intermolecular interactions are treated with empirical force fields) followed by two QM calculations of the central water surrounded by the solvent water molecules represented by point charges. The SPC/E model¹⁷ was used for all molecules, except that, for the reference water, the Coulomb parameters of the Lennard-Jones-Coulomb potential were obtained from a CHelpG (CHarges from Electrostatic Potentials using a Grid based method) fit¹⁸ of ab initio calculations performed at each step.

The simulations were performed using the MC Metropolis method, implemented in the DICE program.¹⁹ During the simulations, all the water molecules are kept rigid. For the solute water, this is required for the relaxation process, as

discussed below, whereas for the solvent molecules, neglecting the internal modes is assumed to be a good approximation. After each MC run, a representative ensemble of configurations was used to generate an average solvent potential to be included in the solute Hamiltonian, in the form of the ASEC, described elsewhere.¹³ The ASEC is then used in the QM calculations mentioned above. ASEC is a configuration variant of the successful ASEP developed by Aguilar and co-workers²⁰ in which we apply a statistical analysis to make the implementation of the average field of the solvent simpler.

The relaxation process is done by combining the free energy gradient method¹² with the ASEC¹³ approach, in a similar way to that of Galván et al.²¹ It is important to stress that the free energy in question here is the solvent free energy. In the first QM calculation, we obtain the ensemble average of the gradient (forces) and second derivatives (Hessian matrix) of the total energy of the central water in the electrostatic field of the solvent molecules. Therefore, the coordinates of the central water must be fixed during the simulation. With first and second derivatives, we are able to apply a quasi-Newton method (here we used the BFGS algorithm²²) to find a new molecular geometry in the path to the minimum free energy conformation.

In the second QM calculation, we obtain the ensemble average electron distribution of this new molecular geometry in the presence of the solvent water molecules. Thus we fit point charges and point dipoles in the atomic sites of the central water to represent the solute multipole moments. The use of point dipoles, in addition to atomic charges, aims at a more accurate description of the charge distribution of the reference water molecule, and therefore enhance the quality of the solute–solvent interaction potential.

The updated molecular geometry and charge distribution are then used in a new MC simulation, initiating the next step of the iterative relaxation process.

3. CALCULATION DETAILS

At each simulation step, we performed 4 MC runs starting from different random configurations. In each MC run, after 75×10^6 equilibration steps (25×10^6 in NVT followed by 50×10^6 in NPT) we performed a NPT production simulation of 100×10^6 steps. From each of the four simulations, we extracted 100 statistically uncorrelated configurations, using standard procedures,²³ resulting in 400 statistically relevant configurations. The aim of such procedure is to accelerate the simulation step by performing smaller simulations in parallel and, at the same time, to improve the sampling of the configuration space, thus enhancing the statistical convergence of the molecular properties.

The QM calculations were performed with the Gaussian program.²⁴

4. RESULTS AND DISCUSSION

4.1. Electronic Structure of Gas-Phase Water. First, we chose a calculation level to describe the electronic structure of the reference water molecule for the relaxation process. The chosen calculation method must accurately describe the dipole moment and the dipole polarizability so as to describe correctly, at any step, the electronic distribution of the molecule. As we are also relaxing the geometry of the molecule, the calculation level must also accurately describe the gas-phase equilibrium geometry and the derivatives of the energy with respect to

nuclear displacement. The accuracy of the derivatives was checked by calculating the vibrational frequencies.

As Table 1 shows, all methods give very good geometries for water, compared to the experimental values.^{25,26} Comparing

Table 1. Geometric Parameters (Distances in Å, Angles in Degrees) and Dipole Moment (μ in D) of Isolated Water

method	R(O–H)	θ (H–O–H)	μ
MP2/cc-pVQZ	0.9577	104.0	1.909
MP2/cc-pVSZ	0.9579	104.3	1.898
MP2/aug-cc-pVQZ	0.9589	104.3	1.862
MP2/aug-cc-pVSZ	0.9584	104.3	1.864
CCSD(T)/cc-pVQZ	0.9579	104.1	2.015
CCSD(T)/cc-pVSZ	0.9580	104.4	2.005
experiment	0.9575^a 0.9584^b	104.5^a	1.855^c

^aReference 25. ^bReference 26. ^cReference 27.

MP2 and CCSD(T) results with equal basis sets, we find differences on the order of 10^{-4} Å for the O–H bond length and 0.1° for the H–O–H angle. However, dipole moments predicted by CCSD(T) seem to be a little overestimated, probably because of the lack of diffuse functions in the basis set. Considering all those aspects, a very good compromise between accuracy and feasibility was found by using the MP2/aug-cc-pVSZ level. The dipole moment obtained at this level is 1.864 D, very close to the experimental value of 1.855 D.²⁶ The dipole polarizability is calculated as 9.69 au, again, very close to the experimental range of 9.79–9.83 au.^{25,28}

The calculated vibrational frequencies for isolated water are also in very good agreement with the experimental values as shown in Table 2. Here we must point out that water has a

Table 2. Harmonic (Anharmonic in Parentheses) Vibrational Frequencies (cm^{-1}) of Isolated Water

method	ν_1 (symm. str.)	ν_2 (bend)	ν_3 (asymm. str.)
MP2/aug-cc-pVTZ	3861 (3694)	1619 (1568)	3988 (3809)
MP2/aug-cc-pVQZ	3846 (3674)	1631 (1578)	3972 (3788)
MP2/aug-cc-pVSZ	3843	1632	3969
experiment^a	3657	1595	3756

^aReference 30.

significant anharmonic character. Therefore, a correction is necessary to quantitatively compare with experimental values. Such anharmonic corrections are done at second-order perturbation theory level²⁹ and are not feasible for the aug-cc-pVSZ basis set. However, harmonic frequencies agree within 3 cm^{-1} using either aug-cc-pVQZ or aug-cc-pVSZ. In fact, only little improvement is observed, for all properties, when going from quadruple- to quintuple- ζ basis set. Therefore we used the quadruple- ζ basis set for calculating all the vibrational frequencies in the present work. At such level, anharmonic frequencies are calculated as 1578, 3674, and 3788 cm^{-1} , respectively, for the ν_2 (bending), ν_1 (symmetric stretching), and ν_3 (asymmetric stretching) modes, in good agreement with the experimental³⁰ peak values of 1595, 3657, and 3756 cm^{-1} .

We conclude that MP2/aug-cc-pVSZ is a very good QM model to perform both the electronic polarization and geometry relaxation of the water molecule, giving a sufficiently accurate electronic distribution for the purposes of the present work.

Those results are further complemented with calculations of the NMR parameters of in vacuo water, namely, σ , the magnetic shielding, and J , the SSCC. NMR properties are very sensitive to the chemical environment of atoms and have been largely used to experimentally investigate the structure of molecules and biomolecules.³¹

To calculate the NMR properties of water, we used the hybrid GGA density functional B3LYP³² with the Jensen's basis sets pcS^{33a} and pcJ^{33b} optimized to density functional calculations of magnetic properties. B3LYP has been largely used to calculate, with relative success, a variety of electronic properties of molecules, but it has been shown by Keal et al.³⁴ that other functionals have more consistent performance for SSCC calculations. However, their results suggest that for couplings involving N, O, and H atoms, B3LYP gives consistently good results and, specifically for H_2O and NH_3 , B3LYP gives better results than other, more recent, functionals. Our best values are obtained with B3LYP/aug-pcS-3 for magnetic shielding (Table 3) and B3LYP/aug-pcJ-3 for SSCC

Table 3. Magnetic Shieldings (ppm) of Isolated Water

method	$\sigma^{\text{iso}}(^{17}\text{O})$	$\sigma^{\text{anis}}(^{17}\text{O})$	$\sigma^{\text{iso}}(^1\text{H})$	$\sigma^{\text{anis}}(^1\text{H})$
MP2/aug-cc-pVTZ	345.9	44.4	30.8	20.5
MP2/aug-cc-pVQZ	345.9	45.2	30.5	20.9
B3LYP/aug-cc-pVTZ	327.7	54.0	31.3	19.3
B3LYP/aug-pcS-2	327.8	56.1	31.1	19.6
B3LYP/aug-pcS-3	326.1	55.6	31.0	19.7
experiment^a	323.6^b		30.2^c	19.1^c

^aOur calculated values are not vibrationally corrected and therefore cannot be directly compared to experimental values (see text). Negative ZPV corrections are estimated (ref 40) to be in the range 4–12 ppm for $\sigma^{\text{iso}}(^{17}\text{O})$ and 0.05–0.5 ppm for $\sigma^{\text{iso}}(\text{H})$. ^bReference 36. ^cReference 37.

Table 4. SSCCs (Hz) for Isolated Water

method	$^1J(^{17}\text{O},\text{H})$	$^2J(\text{H},\text{H})$
B3LYP/aug-pcJ-2	−76.8	−7.20
B3LYP/aug-pcJ-3	−77.0	−7.38
experiment^a	−78.7^b	−7.34^c

^aOur calculated values are not vibrationally corrected and therefore cannot be directly compared to experimental values (see text). ZPV corrections are estimated (ref 41) to be in the range 4–5 Hz for $^1J(^{17}\text{O},\text{H})$ and $\sim 1 \text{ Hz}$ for $^2J(\text{H},\text{H})$. ^b H_2O in cyclohexane (ref 38). ^c H_2O in nitromethane (ref 39).

(Table 4). The two basis sets are of quadruple- ζ type, and they differ mostly on the description of the electron density in the region near the nuclei. The pcJ- n sets include primitive gaussians with higher exponents, tightly bound to the nucleus, that are important to obtain accurate values for the Fermi Contact term.³⁵

From Tables 3 and 4 we observe that only little improvement is obtained from the triple- to the quadruple- ζ basis set, suggesting that the values obtained are converged. The calculated magnetic shieldings are in very good agreement with experiment.^{36,37} The proton shielding is overestimated by only $\sim 1 \text{ ppm}$, and the oxygen shielding by $\sim 3 \text{ ppm}$. The calculated SSCCs are also in very good agreement with experiment.^{38,39} Our calculated $^1J(^{17}\text{O},\text{H})$ value is overestimated by only 1.7 Hz, and our $^2J(\text{H},\text{H})$ value is essentially

equal to the experimental value. However, our calculated NMR properties are not vibrationally corrected and therefore cannot be directly compared to experiment, as magnetic shielding constant and SSCC are geometry-sensitive properties.

For magnetic shielding constants, zero-point vibrational (ZPV) corrections were estimated by Vaara et al.,^{40a} Wigglesworth et al.,^{40b} and Ruud et al.^{40c} using MCSCF, and they found negative corrections of 10–12 ppm for the oxygen shielding and 0.5 ppm for the proton shielding. More recently, Sabzyan and Buzari^{40d} estimated those corrections to be, respectively, −4 ppm and −0.05 ppm, using B3LYP. Those estimations show that the ZPV correction is not negligible for the oxygen shielding, but, after adding them, our results are still in very good agreement with the experimental values. As for the SSCCs, Wigglesworth et al.^{41a} estimated, using high-level quantum chemistry calculations, that the ZPV correction for $^1J(^{17}\text{O},\text{H})$ in water is ~ 4 Hz, while for $^2J(\text{H},\text{H})$ it is ~ 1 Hz, and both corrections are positive. Ruden et al.^{41b} estimated the corrections to be ~ 5 Hz for $^1J(^{17}\text{O},\text{H})$ and ~ 1 Hz for $^2J(\text{H},\text{H})$ using B3LYP. On the basis of those corrections, our values are in fact overestimated by 6–7 Hz for $^1J(^{17}\text{O},\text{H})$ and by ~ 1 Hz for $^2J(\text{H},\text{H})$. Nevertheless, the agreement with experiment is still good, and it corroborates that B3LYP is a good choice for calculating magnetic properties of water.

4.2. Water in Liquid Environment. Initially, let us discuss the geometry relaxation process. Figure 1 shows the evolution

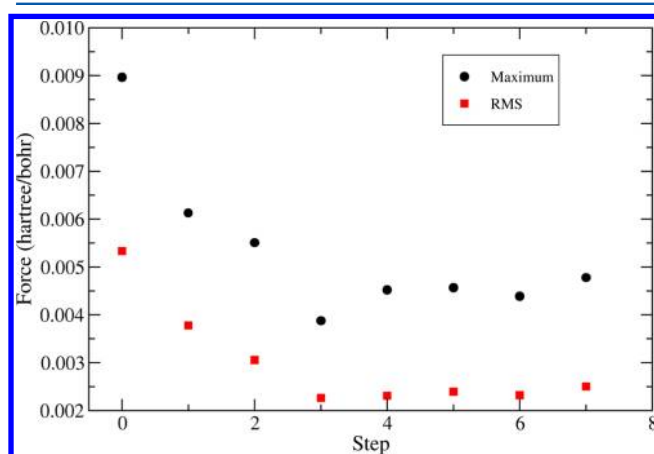


Figure 1. Evolution of the force on the atoms. The maximum and the rms of the nine components are shown.

of the root-mean-square (rms) and the maximum component of the force in the atoms of the reference water molecule. The forces are all within the order of 10^{-3} hartree/bohr (atomic unit) because the relaxation of water is relatively small. The expected increase in the O–H bond length from experiments^{10,25,26} is 0.012 ± 0.005 Å. The rms force starts at 0.0055 au and after 3 steps it goes down to a plateau at 0.0025 au. This is around 6 times the usual threshold for gas-phase geometry optimizations, but, as pointed out by Nagaoka and co-workers,¹² fluctuations due to the dynamics of the liquid prevent one from reaching force magnitudes on the order of those obtained in gas-phase calculations. More important, however, is to observe the evolution of the geometrical parameters that arise from those forces. Figure 2 shows the O–H bond length values with the relaxation step. The two O–H bonds increase fairly symmetrically, as a result of using an average solvent electrostatic field. This is in accord with the

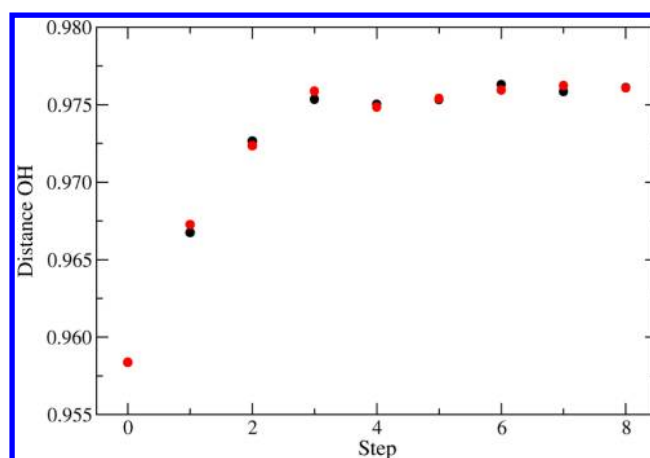


Figure 2. Evolution of the two O–H distances. Note that the O–H bonds are fairly symmetric, which is expected for average forces. After the third iteration step, the distance starts to fluctuate around an equilibrium value (0.976 Å). The experimental estimate is $R(\text{O–H}) = 0.970 \pm 0.005$ Å (ref 10).

expectation that, despite having different instantaneous values, the two bonds have equal lengths in average. We also observe that after step 3, the O–H bond length fluctuates between 0.975 and 0.977 Å. Our converged in-liquid O–H bond length is then 0.976 ± 0.001 Å. This value is in excellent agreement with the neutron diffraction experimental¹⁰ value of 0.970 ± 0.005 Å. Nymand and Åstrand,⁵ using a Sequential QM/MM procedure, found exactly the same value for the equilibrium O–H bond length in liquid water at 300 K, using a CASSCF wave function to treat the central water molecule.

The H–H distance, whose values along the relaxation are shown in Figure 3, also fluctuates around an equilibrium value,

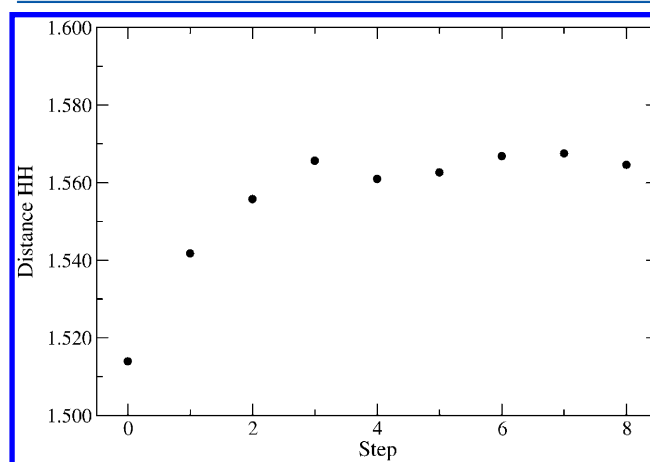


Figure 3. Evolution of H–H distance. From the third step it oscillates around the equilibrium value (1.565 Å). The experimental estimate is $R(\text{H–H}) = 1.55 \pm 0.01$ Å (ref 10). Our H–O–H equilibrium angle is 106.6° .

and the converged distance is 1.565 ± 0.005 Å. This is also in good agreement with the experimental¹⁰ value of 1.55 ± 0.01 Å. Our equilibrium H–O–H angle is then 106.6° , corresponding to a small increase of 2.3° .

In contrast to the subtle change in the geometry, the electronic polarization of water is pronounced. Again, after step 3, the dipole moment fluctuates around 2.72 D, as shown in Figure 4. Although there is no direct experimental measure-

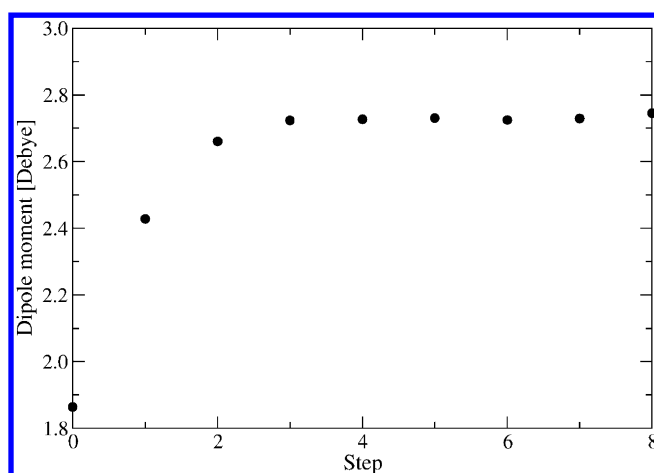


Figure 4. Evolution of the dipole moment of the central water molecule. It also oscillates around the equilibrium value (2.72 D) after the third step.

ment of the in-liquid dipole moment of water, there is a range of 2.4–3.0 D calculated in the literature,¹¹ including estimates from both theoretical and experimental results. Our result lies within this range. The present value of 2.72 D is consistent with the dielectric constant of water and very close to some previous theoretical determinations.^{7,42}

Table 5 summarizes all these results and compares with other theoretical calculations in the literature. Our in-liquid average

Table 5. Equilibrium Geometric Parameters (Distances in Å, Angles in Degrees) and Dipole Moment (μ in D) of Water in a Liquid Environment^a

	this work	other theoretical works			experiment ^b
$R(\text{O}-\text{H})$	0.976	0.951 ^c	0.976 ^d	1.001 ^e	0.970 ± 0.005
ΔR	0.018	0.010 ^c	0.018 ^d	0.027 ^e	0.012 ± 0.006
$\theta(\text{H}-\text{O}-\text{H})$	106.6	110.2 ^c	105.3 ^d		106.1
$\Delta\theta$	2.3	4.0 ^c	0.5 ^d		1.5
μ	2.72	2.88 ^c		2.92 ^e	
$\Delta\mu$	0.86	0.82 ^c		0.82 ^e	

^aThe gas-to-liquid shift, ΔX , of each property is also reported.

^bReferences 10, 25, and 26. ^cConventional QM/MM using MC and HF (refs 4 and 8e). ^dSequential QM/MM using MD and CASSCF (ref 5). ^eConventional QM/MM using MD and DFT (ref 7).

geometric parameters for the water molecule are in very good agreement with experimental data and represent some improvement over previous theoretical works.

Table 6 shows the values of the vibrational frequencies of the reference water molecule in liquid environment. The frequencies are obtained by calculating the Hessian of the relaxed central water, embedded in the solvent molecules represented by the ASEC mean field, and including anharmonic correction afterward.²⁹ We calculated the frequencies for steps 3–7, which correspond to equilibrium geometries, and then obtained the average values. Note that our approach can only provide mean, static values for the vibrational frequencies. This calculation cannot account for the diversity of frequencies related to all the different situations in which the water molecules are to be found in the liquid, with different numbers of hydrogen bonds (HBs), for example. Having clarified this point, we discuss the results for the vibrational frequencies.

Table 6. Anharmonic Vibrational Frequencies (cm^{-1}) Calculated with MP2/aug-cc-pVQZ for the Reference Water Molecule in a Liquid Environment Using ASEC

Step	ν_1 (symm. str.)	ν_2 (bending)	ν_3 (asymm. str.)
3	3428	1675	3461
4	3435	1676	3467
5	3436	1687	3454
6	3428	1683	3446
7	3429	1686	3445
average	3431	1681	3455
experiment ^a	3390–3423	1645	3511–3535
shift (this work)	−243	103	−333
shift (literature) ^b	−423	−41	−405
exp. shift	−267 to −234	50	−245 to −221

^aReferences 42 and 43. ^bReference 5.

The average in-liquid symmetric stretching frequency of 3431 cm^{-1} is in very good agreement with the experimental range^{43,44} of $3390\text{--}3423 \text{ cm}^{-1}$. The bending frequency is calculated as 1681 cm^{-1} , slightly overestimated compared to the experimental value of 1645 cm^{-1} , but still in good agreement. The frequency for the asymmetric stretching is calculated as 3455 cm^{-1} on average, close to the experimental range⁴⁴ of $3511\text{--}3535 \text{ cm}^{-1}$. Regarding the gas-to-liquid shift of the frequencies, the calculated symmetric stretching is shifted by 243 cm^{-1} , in excellent agreement with the experimental range of $234\text{--}267 \text{ cm}^{-1}$. As for the asymmetric stretching and bending modes, the calculated frequencies are red-shifted by 333 cm^{-1} and blue-shifted by 103 cm^{-1} , respectively. Both results give the right direction for the shift, but are somewhat overestimated as compared to the experimental values of $221\text{--}245 \text{ cm}^{-1}$ for the stretching and 50 cm^{-1} for the bending. The experimental frequency for the asymmetric mode is in fact an estimate, because it cannot be obtained directly from the spectra. The stretching modes are active in IR, and the two bands overlap. Together with an overtone of the bending mode, they give rise to a single and broad band, from which it is difficult to extract the individual bands. In the Raman spectrum, on the other hand, the symmetric stretching gives a pronounced peak, but the asymmetric stretching has a very small intensity because the polarizability variation is smaller for this mode. Therefore, the experimental value for the symmetric mode is obtained from a direct measurement, but for the asymmetric it is based on an estimate using the second difference method.⁴⁴ Our results suggest that the experimental gas-to-liquid shift may be slightly larger than the value inferred. In spite of the very good in-liquid water geometry obtained by Nyman and Åstrand⁵ as discussed before and shown in Table 5, they found considerably larger (in magnitude) frequency shifts for the stretching modes and a small shift, but in the opposite direction, for the bending mode. This may be explained, in part, because they used a solvent perturbation from a simulation performed with the rigid gas-phase water molecules. Therefore, the surrounding ambient of the reference water molecule was not accurately in equilibrium with the relaxed water geometry. Another possible source of inaccuracy is the harmonic approximation used in their work.

To further analyze the quality of the description of the geometry and electronic structure of the relaxed water molecule, we also calculated the magnetic shielding and SSCs of the central water in liquid environment.

First, let us discuss the results for the in-liquid magnetic shielding and the gas-to-liquid chemical shift. For the chemical shift, the vibrational correction discussed above must have limited impact, since they must be mostly canceled. By representing the solvent water molecules using only the ASEC, we found a downfield shift of around 17 ppm for $\sigma^{\text{iso}}(^{17}\text{O})$, therefore in the opposite direction of the experimental shift. This shows the necessity of employing a wave function representation of the electronic distribution of the neighboring water molecules, which leads to wave function delocalization over the solvent region. This is possibly the major reason for the poor agreement with experiment obtained by Nyman and Åstrand⁶ for the chemical shift of $\sigma^{\text{iso}}(^{17}\text{O})$, as they do not employ a wave function description for the neighboring waters.

Therefore we calculated, for each step, the average of the shieldings over 100 uncorrelated configurations (25 from each of the four parallel runs) of 5 QM waters (central plus the four nearest) embedded in a background of point charges representing the remaining water molecules up to 12 Å away. The basis set used consists of aug-pcS-2 for the central water and pcS-2 for the other four. By finally averaging over steps 3–7, we obtain the values shown in Table 7.

Table 7. Magnetic Shieldings (ppm) for Liquid Water Calculated with B3LYP Using an Explicit Water Shell around the Central Water

	$\sigma^{\text{iso}}(^{17}\text{O})$	$\sigma^{\text{anis}}(^{17}\text{O})$	$\sigma^{\text{iso}}(\text{H})$	$\sigma^{\text{anis}}(\text{H})$
calculated ^a	268.9	33.5	24.7	30.1
experiment	287.5 ^b		25.7 ^c	27.4 ^c
calc. shift	−58.9	−22.6	−6.4	10.5
exp. shift	−36.1		−4.5	8.3

^aAverage of the shieldings calculated in steps 3–7. The shielding calculated in each step is, in turn, the average over 100 uncorrelated configurations of five explicit waters embedded in the background of point charges. The basis set is aug-pcS-2 for central water and pcS-2 for the remaining four waters (see text). ^bReference 36. ^cReference 37.

We observe that, in particular, the shifts of $\sigma^{\text{iso}}(\text{H})$ and $\sigma^{\text{anis}}(\text{H})$ are small, and the calculated shifts are in very good agreement with experiment, both with the magnitude overestimated by only ~2 ppm. The upfield shift of $\sigma^{\text{iso}}(^{17}\text{O})$ calculated as 58.9 ppm is now in the right direction, but it is substantially overestimated as compared to the experimental³⁶ value of 36 ppm.

Now, two aspects should be considered regarding comparison of chemical shifts with the experimental values. First, it is more difficult to guarantee convergence with respect to the number of QM water molecules because the computational cost increases prohibitively for larger QM aggregates. Nevertheless, we assume that the main effect comes from the four nearest neighbors, which make HBs with the central water. Second, other effects should be considered to improve the description of the chemical environment of the central water, as we shall discuss shortly. Thus, we are satisfied, for the present work, with the agreement obtained for the absolute magnetic shieldings and chemical shifts.

To analyze the geometrical and electronic structure of the central water, a more important observable is the SSCC J , because it is more sensitive to the geometry of the molecule and its electronic distribution. Table 8 shows the calculated average values of $^1J(^{17}\text{O},\text{H})$ and $^2J(\text{H},\text{H})$ for the central water.

Table 8. SSCCs (Hz) Calculated with B3LYP/aug-pcJ-3 for Water in a Liquid Environment Obtained Using ASEC

	$^1J(^{17}\text{O},\text{H})$	$^2J(\text{H},\text{H})$
calculated ^a	−88.1	−6.7
experiment ^b	−89.8 ± 2.3	
calc. shift	−11.1	0.7
exp. shift	−11.1 ± 2.3	

^aAverage of the SSCCs calculated in steps 3–7. ^bReference 45.

The shown values were obtained by simply employing the ASEC (built using the 400 uncorrelated configurations) to calculate the average constants for each step and then averaging over steps 3–7. We found that using the ASEC is enough to accurately calculate the SSCC. The QM description of the four nearest water molecules implies a difference of only ~0.5 Hz. The calculated average value of $^1J(^{17}\text{O},\text{H})$ for the in-liquid water is −88.1 Hz and is in very good agreement with the experimental⁴⁵ value of −89.8 ± 2.3 Hz. Again, this value cannot be directly compared to the experimental value and, by including the vibrational correction, our result is actually 6–7 Hz overestimated. However, the shift may be compared directly with experiment, as the vibrational correction for the relaxed water must be similar to the gas-phase situation and therefore they are likely to be mostly canceled when giving the gas-to-liquid shift. Our shift is calculated as −11.1 Hz and is in sharp agreement with the experimental value of −11.1 ± 2.3 Hz. This result strongly corroborates that our description of the equilibrium structure of in-liquid water is very good, and the methodology used is capable of giving accurate optimized molecular geometries in medium.

Let us now look at the solute–solvent structure. Table 9 shows the number of HBs formed between the reference water

Table 9. Average Number of HBs between the Reference Water and Solvent Waters^a

step	accepting	donating	total
0	1.6	1.6	3.2
1	2.3	1.9	4.2
2	2.5	2.0	4.5
3	2.5	1.9	4.5
4	2.6	2.0	4.5
5	2.5	2.0	4.5
6	2.6	2.0	4.6
7	2.6	2.0	4.6

^aCriteria: $R(\text{O}–\text{O}) \leq 3.5$ Å; $\theta(\text{O}–\text{O}–\text{H}) \leq 40^\circ$; $E_{\text{bond}} \geq 2.0$ kcal/mol.

molecule and the solvent molecules. Standard fixed criteria [$R(\text{O}–\text{O}) \leq 3.5$ Å; $\theta(\text{O}–\text{O}–\text{H}) \leq 40^\circ$; $E_{\text{bond}} \geq 2.0$ kcal/mol] were used for all steps. Those criteria closely match the ones used in the literature.⁴⁶ The HB definition is not unique, although they usually respect some energetic^{47a} and geometric^{47b} directives. This is because, in fact, there is a whole spectrum of possible HBs varying in intensity, from the weakest to the strongest. On the other hand, the number of HBs is not significantly altered by small variations in the criteria.

We observe that already in the second step the total number of HBs is a little over 4, indicating a strong interaction between the central water and the neighboring ones. In the equilibrium, the central water forms, on average, 4.6 HBs with the solvent water, a little more than the expected maximum of 4 HBs which

corresponds to the tetrahedral picture of ice. Although locally overstructured water is sometimes reported, with some molecules making 5 HBs,⁴⁸ the average number of HBs reported in the literature is generally below 4.^{46b,49} As we can see in Table 9, the exceeding number of HBs comes entirely from the bonds between the oxygen of central water and the hydrogen of solvent water molecules. This is most probably the reason behind the overestimation of the chemical shift of the oxygen of the central molecule, as reported above.

Now, the increased number of HBs is probably due to a little overpolarization of the central water, which takes place as a result of some misbalancing of the LJ and the Coulomb parts of the intermolecular potential. The refinement of the Coulomb parameters, that is, the atomic charges, is important to improve the intermolecular interaction, mainly for polar systems. However, as pointed out before,⁵⁰ a reparameterization of the LJ part of the potential is necessary for further refinement of the intermolecular potential to describe nonlocal and bulk properties.

Nevertheless, the local properties are in very good agreement with experimental data, and the employed methodology is capable of giving accurate relaxed geometries, electronic distribution, and related magnetic properties.

5. CONCLUSION

There is a continuous need for improving methodologies to deal with the electronic properties of homogeneous liquids and solvent effects. The free energy gradient method is an important avenue that accommodates the possibility of including the geometry relaxation and electronic solute polarization. Previous applications of the free energy method, although successful in some aspects, were incomplete in assessing its potential accuracy. In this work, the combination of the sequential QM/MM methodology and the free energy gradient method is used with high-level QM methods to obtain very accurate values for the geometry, dipole moment, dipole polarizability, NMR chemical shift, and SSCC. All results are found to be in very good agreement with experiment, thus corroborating that the methodology is able to provide accurate values for the electronic properties of in-liquid water.

AUTHOR INFORMATION

Corresponding Author

*E-mail: hcgeorg@ifufg.br. Tel/Fax: +55 62 3521-1014.

Notes

The authors declare no competing financial interest.

ACKNOWLEDGMENTS

We acknowledge the financial support from the agencies FAPESP, CNPq, and FAPEG and from the NBionet-Brasil collaboration. We thank Dr. K. Coutinho for discussion and assistance and the computer resources of IFUSP and LCC-IFUFG laboratories.

REFERENCES

- (1) Maréchal, Y. *Hydrogen Bond and the Water Molecule: The Physics and Chemistry of Water, Aqueous and Bio-Media*; Elsevier: Amsterdam, 2007.
- (2) See the special issue "Combined QM/MM Calculations in Chemistry and Biochemistry", *J. Mol. Struct. (THEOCHEM)* **2003**, 632, edited by Ruiz-López, M. F.

- (3) See the issue "Combining Quantum Mechanics and Molecular mechanics: Some Recent Progresses in QM/MM Methods", *Adv. Quantum Chem.* **2010**, 59, edited by Canuto, S.
- (4) Moriarty, N. W.; Karlström, G. *J. Chem. Phys.* **1997**, 106, 6470–6474.
- (5) Nyman, T. M.; Åstrand, P.-O. *J. Phys. Chem. A* **1997**, 101, 10039–10044.
- (6) (a) Nyman, T. M.; Åstrand, P.-O.; Mikkelsen, K. V. *J. Phys. Chem. B* **1997**, 101, 4105–4110. (b) Nyman, T. M.; Åstrand, P.-O. *J. Chem. Phys.* **1997**, 106, 8332–8338.
- (7) Chalmet, S.; Ruiz-López, M. *J. Chem. Phys.* **2001**, 115, 5220–5227.
- (8) (a) Millot, C.; Cabral, B. J. C. *Chem. Phys. Lett.* **2008**, 460, 466–469. (b) Osted, A.; Kongsted, J.; Mikkelsen, K. V.; Åstrand, P.-O.; Christiansen, O. *J. Chem. Phys.* **2006**, 124, 124503-1–16. (c) Rocha, W. R.; Coutinho, K.; de Almeida, W. B.; Canuto, S. *Chem. Phys. Lett.* **2001**, 335, 127–133. (d) Tu, Y.; Laaksonen, A. *J. Chem. Phys.* **2000**, 113, 11264–11269. (e) Moriarty, N. W.; Karlström, G. *J. Phys. Chem.* **1996**, 100, 17791–17796.
- (9) Åstrand, P.-O.; Linse, P.; Karlström, G. *Chem. Phys.* **1995**, 191, 195–202.
- (10) Ichikawa, K.; Kameda, Y.; Yamaguchi, T.; Wakita, H.; Misawa, M. *Mol. Phys.* **1991**, 73, 79–86.
- (11) Gubskaya, A. V.; Kusalik, P. G. *J. Chem. Phys.* **2002**, 117, 5290–5302 and references therein.
- (12) (a) Okuyama-Yoshida, N.; Nagaoka, M.; Yamabe, T. *Int. J. Quantum Chem.* **1998**, 70, 95–103. (b) Okuyama-Yoshida, N.; Kataoka, K.; Nagaoka, M.; Yamabe, T. *J. Chem. Phys.* **2000**, 113, 3519–3524. (c) Hirao, H.; Nagae, Y.; Nagaoka, M. *Chem. Phys. Lett.* **2001**, 348, 350–356.
- (13) Coutinho, K.; Georg, H. C.; Fonseca, T. L.; Ludwig, V.; Canuto, S. *Chem. Phys. Lett.* **2007**, 437, 148–152.
- (14) Gester, R. M.; Georg, H. C.; Canuto, S.; Caputo, M. C.; Provasi, P. F. *J. Phys. Chem. A* **2009**, 113, 14936–14942.
- (15) (a) Georg, H. C.; Coutinho, K.; Canuto, S. *Chem. Phys. Lett.* **2006**, 429, 119–123. (b) Georg, H. C.; Coutinho, K.; Canuto, S. *J. Chem. Phys.* **2007**, 126, 034507-1–8.
- (16) Coutinho, K.; Rivelino, R.; Georg, H. C.; Canuto, S. In *Solvation Effects in Molecules and Biomolecules. Challenges and Advances in Computational Chemistry and Physics*; Canuto, S., Ed.; Springer: London, 2008; Vol. 6, pp 159–189.
- (17) Berendsen, H. J. C.; Grigera, J. R.; Straatsma, T. P. *J. Phys. Chem.* **1987**, 91, 6269–6271.
- (18) Breneman, C. M.; Wiberg, K. B. *J. Comput. Chem.* **1990**, 11, 361–373.
- (19) Coutinho, K.; Canuto, S. *DICE: A Monte Carlo Program for Molecular Liquid Simulation*, version 2.9; Universidade de São Paulo: São Paulo, Brazil, 2009.
- (20) (a) Sánchez, M. L.; Aguilar, M. A.; Olivares del Valle, F. J. *J. Comput. Chem.* **1997**, 21, 313–322. (b) Sánchez, M. L.; Martín, M. E.; Aguilar, M. A.; Olivares del Valle, F. J. *J. Comput. Chem.* **2000**, 21, 705–715. (c) Martín, M. E.; Sánchez, M. L.; Olivares del Valle, F. J.; Aguilar, M. A. *J. Chem. Phys.* **2002**, 116, 1613–1620.
- (21) Galván, I. Fdez.; Sánchez, M. L.; Martín, M. E.; Olivares del Valle, F. J.; Aguilar, M. A. *J. Chem. Phys.* **2003**, 118, 255–263.
- (22) (a) Broyden, C. G. *J. Inst. Math. Appl.* **1970**, 6, 76–90. (b) Fletcher, R. *Comput. J.* **1970**, 13, 317–322. (c) Goldfarb, D. *Math. Comput.* **1970**, 24, 23–26. (d) Shanno, D. F. *Math. Comput.* **1970**, 24, 647–656.
- (23) Malaspina, T.; Coutinho, K.; Canuto, S. *J. Chem. Phys.* **2002**, 117, 1692–1699.
- (24) Frisch, M. J.; Trucks, G. W.; Schlegel, H. B.; Scuseria, G. E.; Robb, M. A.; Cheeseman, J. R.; Scalmani, G.; Barone, V.; Mennucci, B.; Petersson, G. A. et al. *Gaussian 09*, revision A.02, Gaussian Inc.: Wallingford, CT, 2009.
- (25) Lide, D. R., Ed., *CRC Handbook of Chemistry and Physics*, 87th ed.; Taylor and Francis: Boca Raton, FL, 2007.
- (26) Benedict, W. S.; Gailar, N.; Plyler, E. K. *J. Chem. Phys.* **1956**, 24, 1139–1165.

- (27) Clough, S. A.; Beers, Y.; Klein, G. P.; Rothman, L. S. *J. Chem. Phys.* **1973**, *59*, 2554–2259.
- (28) Russel, A. J.; Spackman, M. A. *Mol. Phys.* **1995**, *84*, 1239–1255.
- (29) (a) Barone, V. *J. Chem. Phys.* **2004**, *120*, 3059–3065. (b) Barone, V. *J. Chem. Phys.* **2005**, *122*, 014108–1–10.
- (30) Kjaergaard, H. G.; Henry, B. R.; Wei, H.; Lefebvre, S.; Carrington, T., Jr.; Mortensen, O. S.; Sage, M. L. *J. Chem. Phys.* **1994**, *100*, 6228–6239 and references therein.
- (31) Hore, P. *J. Nuclear Magnetic Resonance*; Oxford University Press: New York, 1995.
- (32) (a) Becke, A. D. *J. Chem. Phys.* **1993**, *98*, 5648–5652. (b) Lee, C.; Yang, W.; Parr, R. G. *Phys. Rev. B* **1988**, *37*, 785–789.
- (33) (a) Jensen, F. *J. Chem. Theory Comput.* **2008**, *4*, 719–727. (b) Jensen, F. *J. Chem. Theory Comput.* **2006**, *2*, 1360–1369.
- (34) Keal, T. W.; Helgaker, T.; Salek, P.; Tozer, D. *J. Chem. Phys. Lett.* **2006**, *425*, 163–166.
- (35) (a) Hameka, H. F. *Advanced Quantum Chemistry*, Addison-Wesley: Reading, MA, 1965. (b) Ramsey, N. F. *Phys. Rev.* **1950**, *78*, 699–703. (c) Ramsey, N. F. *Phys. Rev.* **1953**, *91*, 303–307.
- (36) Wasylishen, R. E.; Bryce, D. L. *J. Chem. Phys.* **2002**, *117*, 10061–10066.
- (37) Modig, K.; Halle, B. *J. Am. Chem. Soc.* **2002**, *124*, 12031–12041.
- (38) Wasylishen, R. E.; Friedrich, J. O. *Can. J. Chem.* **1987**, *65*, 2238–2243.
- (39) (a) Pecul, M.; Sadlej, J. *Chem. Phys. Lett.* **1999**, *308*, 486–494. (b) Sergeev, N. M.; Sergeeva, N. D.; Strelenko, Yu. A.; Raynes, W. T. *Chem. Phys. Lett.* **1997**, *277*, 142–146.
- (40) (a) Vaara, J.; Lounila, J.; Ruud, K.; Helgaker, T. *J. Chem. Phys.* **1998**, *109*, 8388–8397. (b) Wigglesworth, R. D.; Raynes, W. T.; Sauer, S. P. A.; Oddershede, J. *Mol. Phys.* **1999**, *96*, 1595–1607. (c) Ruud, K.; Åstrand, P.-O.; Taylor, P. R. *J. Chem. Phys.* **2000**, *112*, 2668–2683. (d) Sabzyan, H.; Buzari, B. *Chem. Phys.* **2008**, *352*, 297–305.
- (41) (a) Wigglesworth, R. D.; Raynes, W. T.; Sauer, S. P. A.; Oddershede, J. *Mol. Phys.* **1998**, *94*, 851–862. (b) Ruden, T. A.; Lutnaes, O. B.; Helgaker, T.; Ruud, K. *J. Chem. Phys.* **2003**, *118*, 9572–9581.
- (42) (a) Silvestrelli, P. L.; Parrinello, M. *Phys. Rev. Lett.* **1999**, *82*, 3308–3311. (b) Tu, Y.; Laaksonen, A. *Chem. Phys. Lett.* **2000**, *329*, 283–288. (c) Poulsen, T. D.; Ogilby, P. R.; Mikkelsen, K. V. *J. Chem. Phys.* **2002**, *116*, 3730–3738. (d) Coutinho, K.; Guedes, R. C.; Cabral, B. J. C.; Canuto, S. *Chem. Phys. Lett.* **2003**, *369*, 345–353.
- (43) (a) Carey, D. M.; Korenowski, G. M. *J. Chem. Phys.* **1998**, *108*, 2669–2675. (b) Schmidt, D. A.; Miki, K. *J. Phys. Chem. A* **2007**, *111*, 10119–10122.
- (44) Walrafen, G. E.; Pugh, E. *J. Solution Chem.* **2004**, *33*, 81–97.
- (45) Burnett, L. J.; Zeltmann, A. H. *J. Chem. Phys.* **1974**, *60*, 4636–4637.
- (46) (a) Luzar, A.; Chandler, D. *Phys. Rev. Lett.* **1996**, *76*, 928–931. (b) Galamba, N.; Cabral, B. J. C. *J. Am. Chem. Soc.* **2008**, *130*, 17955–17960.
- (47) (a) Rahman, A.; Stillinger, F. H. *J. Am. Chem. Soc.* **1973**, *95*, 7943–7948. (b) Mezei, M.; Beveridge, D. L. *J. Chem. Phys.* **1981**, *74*, 622–632.
- (48) For instance, in Møgelhøj, A.; Kelkkanen, A. K.; Wikfeldt, K. T.; Schiøtz, J.; Mortensen, J. J.; Pettersson, L. G. M.; Lundqvist, B. I.; Jakobsen, K. W.; Nilsson, A.; Nørskov, J. K. *J. Phys. Chem. B* **2011**, *115*, 14149–14160.
- (49) For instance, see the following recent reports: (a) Smith, J. D.; Cappa, C. D.; Wilson, K. R.; Messer, B. M.; Cohen, R. C.; Saykally, R. *J. Science* **2004**, *306*, 851–853. (b) Xenides, D.; Randolph, B. R.; Rode, B. M. *J. Mol. Liq.* **2006**, *123*, 61–67. (c) Hakala, M.; Nygård, K.; Manninen, S.; Huotari, S.; Buslaps, T.; Nilsson, A.; Pettersson, L. G. M.; Härmäläinen, K. *J. Chem. Phys.* **2006**, *125*, 084504-1–7. (d) Bukowski, R.; Szalewicz, K.; Groenenboom, G. C.; van der Avoird, A. *Science* **2007**, *315*, 1249–1252. (e) Kühne, T. D.; Krack, M.; Parrinello, M. *J. Chem. Theory Comput.* **2009**, *5*, 235–241.
- (50) (a) Freindorf, M.; Gao, J. L. *J. Comput. Chem.* **1996**, *17*, 386–395. (b) Tu, Y.; Laaksonen, A. *J. Chem. Phys.* **1999**, *111*, 7519–7525.
- (c) Chalmet, S.; Ruiz-López, M. F. *Chem. Phys. Lett.* **2000**, *329*, 154–159. (d) Martín, M. E.; Aguilar, M. A.; Chalmet, S.; Ruiz-López, M. F. *Chem. Phys.* **2002**, *284*, 607–614. (e) Koyano, Y.; Takenaka, N.; Nagakawa, Y.; Nagaoka, M. *Bull. Chem. Soc. Jpn.* **2010**, *83*, 486–494.